Journal of Computer-Aided Molecular Design, 5 (1991) 303–322
ESCOM

J-CAMD 124

A graph-theoretic approach to modeling metabolic pathways

Eric Gifford[a], Mark Johnson[b,*] and Chun-che Tsai[a]

[a]*Department of Chemistry, Kent State University, Kent, OH 44242, U.S.A.*
[b]*Computational Chemistry, The Upjohn Company, Kalamazoo, MI 49001, U.S.A.*

Received 27 July 1990
Accepted 21 December 1990

Key words: Modeling metabolic pathways; Chemical graphs; Artificial intelligence; Transforms

SUMMARY

The metabolic pathways of medazepam, oxazepam, and diazepam were modeled using graph-theoretic transforms which are incorporable into computer-assisted metabolic analysis programs. The information, represented in the form of a graph-theoretic transform kit, which was obtained from these pathways was then used to predict the metabolites of other benzodiazepine compounds. The transform kits gave statistically significant predictions with respect to a statistical method for evaluating the performance of the transform kits.

INTRODUCTION

Metabolic processes affect the efficacy and toxicity of drug therapy in many ways. Metabolic transformations directly affect the clearance rate of a drug and, consequently, the availability of the drug. In other cases, the active agent in a drug therapy is actually a metabolite of the administered drug. This is so by design in the case of 'soft' drugs [1]. In other cases, the metabolite of a drug may be responsible for the toxicity associated with the administered drug. For these reasons, the structural features influencing the metabolism of a drug have long been important to efficient drug design.

Although there is extensive literature on the types of metabolic transformations that might take place and the enzymes responsible for these transformations, there is considerably less known about the structural features that govern the regioselectivity of those transformations that actually do take place [2]. It is natural to expect that, as data on metabolic pathways accumulate, our ability to predict the metabolic fate of a compound should increase, especially if the data exist for a closely related series of compounds [3].

* To whom correspondence should be addressed.

We are initiating an investigation into computer-based approaches to metabolic prediction, despite current pessimism regarding progress in predicting the regiospecificity of metabolic transformations [2,3] for a number of reasons. First, there are numerous cases in which metabolic transformations can be predicted. Thus, it is not a matter of whether or not the metabolic fate of a compound can be predicted, but rather characterizing our ability to predict in a particular molecular context. Second, although in many drug design contexts we would like to know the major metabolite, a simple ranking of the possible metabolic routes in likelihood of occurrence is often helpful. If one's goal is to synthesize and screen potential metabolites for biological activity, such rankings will focus the screening effort on the most likely metabolites. Third, metabolic databases are becoming available [4, 5, F. Darvas, personal communication to M.J.]. The current version of MetabolExpert [5] includes a database of over 300 complete metabolic trees, and efforts are underway to substantially enlarge the database [F. Darvas, personal communication to M.J.]. These databases will permit dramatically enhanced access to large sets of compounds having similar substructural environments associated with the reaction center of a metabolic transformation of interest. Fourth, learning algorithms for modeling the structural features that govern the occurrence and relative rates of chemical transformations [6–10], as well as expert systems that can incorporate these features into their metabolic prediction rules [5,11,12], are becoming available.

In this study, we explore some simple learning rules for modeling metabolic pathways. This simplicity exposes the essential problem in developing learning rules, i.e., that of finding a structural environment that predicts a high percentage of the observed transformations without predicting too many unobserved transformations. At the same time, the rules are powerful enough to result in a model of benzodiazepine metabolism that gives statistically significant predictions and are refined enough to indicate how secondary recognition features might be brought to the attention of the modeler.

It will become evident that more sophisticated learning rules will need to be developed if regiospecific computer-assisted metabolic prediction is to become a reality. The rules presented here, although simple, are general and are not restricted to compounds with a common skeletal structure as is often required by physico-chemical property prediction approaches [13]. The results show that learning rules can be developed which give regiospecific metabolic predictions for selected series of compounds, and suggest that such predictions are extendable to diverse compounds when the learning rules are based on larger and more informative learning sets of metabolic transformations than the small learning set used in this pilot study.

MODELING THE METABOLIC PATHWAYS OF THE BENZODIAZEPINES

The benzodiazepines are a large class of compounds which are used as antianxiety agents [14,15]. These compounds all have the basic ring structure as shown in Fig. 1, with structural variations occurring as substituents on the ring. This class of compounds was determined to have a sufficient number of different compounds with reported metabolic pathways to allow an evaluation of the performance of this method on exogenous metabolism. The structures in this class, although possessing essentially the same ring substructure, exhibit a wide range of substituents.

Our method of modeling chemical transformation pathways requires the development of the transform kit. Here, the transform kit is computed from a 'learning' set of documented metabolic pathways which we call the learning set. The learning set for this study consists of the metabolic

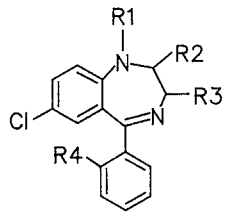

Compound	R1	R2	R3
Medazepam	$-CH_3$	$-H$	$-H$
Diazepam	$-CH_3$	$=O$	$-H$
Oxazepam	$-H$	$=O$	$-OH$

Fig. 1. Basic benzodiazepine ring structure and the three compounds used as learning data.

pathways of medazepam (K), diazepam (L), and oxazepam (M) [16]. These pathways (Fig. 2) are divided into sets each corresponding to a different drug. No compound in any set K, L, or M is considered as a reactant in more than one set. For example, compound K3/L1 is considered as a reactant of only the L set. This distinction provides an unbiased counting of the number of poten-

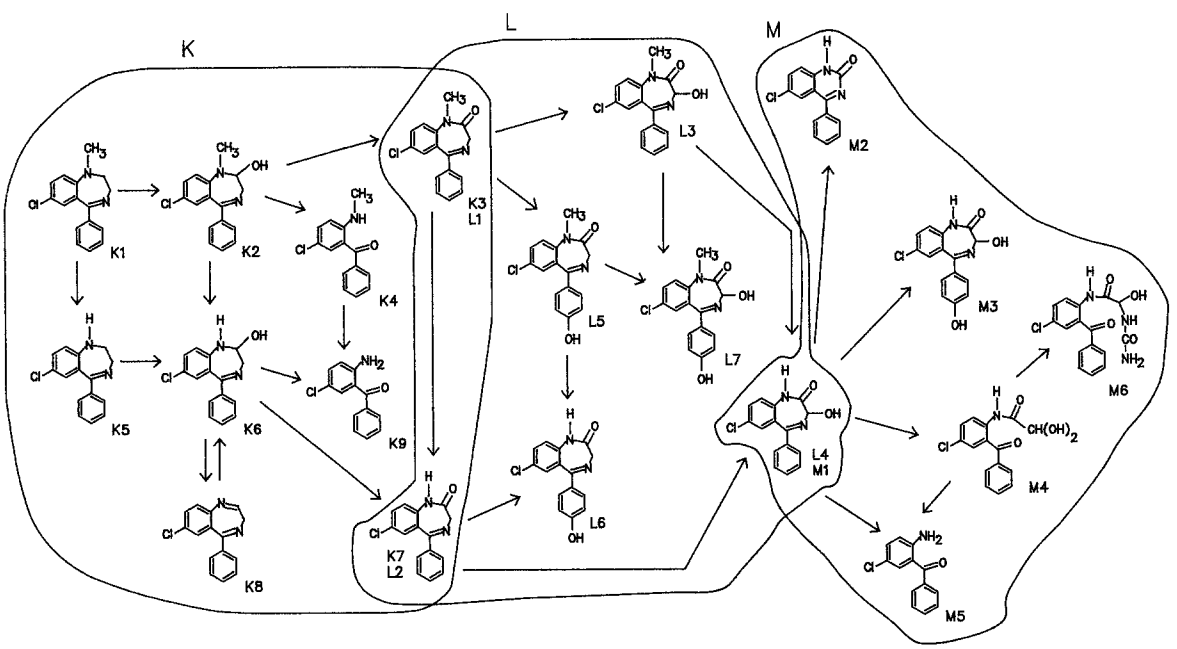

Fig. 2. The metabolic pathways of medazepam (K1), diazepam (L1), and oxazepam (M1), taken from Testa and Jenner [16].

tial reaction sites of a molecule for a given transform as required by our statistical evaluation of the method.

The overall pathway is shown with the circled portions indicating the compounds and specific reaction arrows considered in each set. Each possible pair of pathways (KL, KM, LM) was modeled as learning sets while the remaining pathway was then used as the testing set. The testing set is used to determine how well information obtained from the learning set transformations is represented by a graph transform kit. The development of the transform kit from learning set KL will be given to illustrate the learning algorithm.

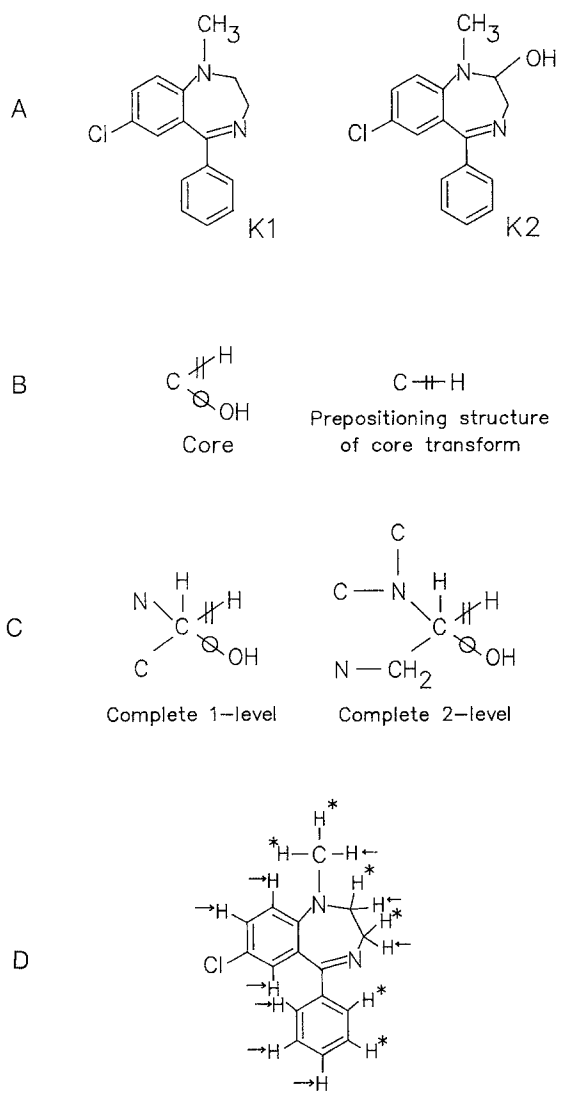

Fig. 3. The local level transforms constructed from the hydroxylation reaction of medazepam. The arrows point to distinguishable action sites of the core transform. Indistinguishable sites are marked with an asterisk.

Graph-theoretic transforms

Every reaction in the learning set will be modeled by a graph transform. The graph transform of a reaction is derived from the superposition of the reactant and product. Using the notation of Fujita [17,18], bonds from the reactant in the superpositioning that are not common to the product are indicated by a double slash and represent bonds which are broken in the transformation. Bonds from the product that are not common to the reactant are indicated by a circle and represent bonds which are formed in the transformation. By deleting all atoms and bonds of the superpositioning except those atoms connected by a slashed or circle bond, we are left with the basic structural change of the transformation. This basic structural change is called the core transform. A core transform is illustrated in Fig. 3B.

The core transform may be extended to a complete 1-level and complete 2-level transform if needed. The complete 1-level transform includes all atoms and bonds (explicit bond types are used) one bond length (connection) away from the core transform. The complete 2-level transform includes all atoms and bonds two bond lengths from the core transform. The complete 1-level and complete 2-level transforms are shown in Fig. 3C. By deleting all atoms and bonds of the transform shared with the product, but not of the reactant, we are left with the prepositioning structure of the transform (the slashed bonds indicate those bonds shared with the reactant, but not the product). The prepositioning structure of the transform is responsible for generating possible reaction sites on a molecule.

For evaluating the predictive performance of a transform, the number of distinguishable reaction sites of a transform must be counted. Since our formalism is based on chemical graphs in which stereoisomers are not distinguished, reaction products differing only in stereochemistry are considered equivalent. For example, the core transform derived from the transformation of K1 to K2 has 9 distinguishable action sites as is indicated by the arrows in Fig. 3D. Those sites indicated by stars indicate alternate action sites which yield products equivalent, according to our criteria, to one of those already indicated by the arrows. In our evaluation, the core transform for the transformation of K1→K2 would have one site on which the transformation actually occurred out of 9 possible position-specific action sites; this is indicated by the ratio 1/9.

Selecting the appropriate transforms

The procedure involved in selecting transforms for inclusion in a transform kit will now be illustrated using several reactions from the KL learning set. Figure 4 shows the transformation of L5 to L6. The core transform for this reaction represents an N-demethylation reaction. The distinguishable action sites of this transform are determined not only for molecule L5 but for every molecule in the learning set being modeled, in this case KL (note that K3 is represented by L1 in this tabulation and that L4 is omitted since L4 is a reactant in the test dataset M). The N-demethylation core transform predicts 6 reactions which are both observed and predicted, as indicated by the ratio 1/1, and one reaction which is predicted but not observed as indicated by 0/1. Overall, for the learning set KL the core transform yields less than 50% false prediction, so it is included in the transform kit.

The next series of reactions examined are all described by the same core transform. The reactions of K1→K2, K5→K6,K3/L1→L3, and K7/L2→L6 all may be represented by the hydroxylation core transform (see Fig. 5A–C). The reaction K1→K2, hydroxylation at the 2-position of the benzodiazepine ring, is modeled using the complete 2-level transform. The reaction of K5 to K6,

hydroxylation at the same position, must also be modeled using a different complete 2-level transform. The difference between these two transforms is seen in the secondary amine (K5→K6) and the tertiary amine (K1→K2). One can take advantage of the obvious commonality between these two transforms to obtain a single, more general transform by superimposing the two transforms and deleting those atoms and bonds which cannot be superimposed. Conditions in which it would be desirable to do so are the subject of another investigation.

The reaction of K7/L2 → L6 cannot be sufficiently modeled (< 50% false prediction) by even the complete 2-level transform (Fig. 5D). In cases such as this, it is necessary to take into account structural features quite removed from the reaction center. For example, in learning set KL para-

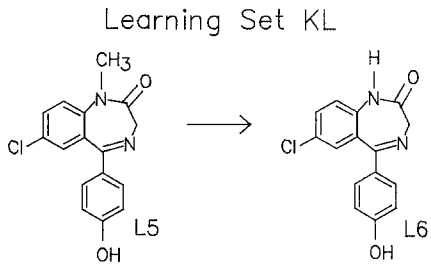

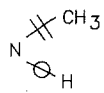

K1	1/1
K2	1/1
K4	1/1
K5	0/0
K6	0/0
K8	0/0
K9	0/0
K Total	3/3
L1	1/1
L2	0/0
L3	1/1
L5	1/1
L6	0/0
L7	0/1
L Total	3/4
KL Total	6/7

Fig. 4. The number of observed/predicted reactions for each reactant molecule in the KL learning dataset based on the core transform constructed from the N-demethylation having L5 as the reactant.

hydroxylation is observed only when a carbonyl group is present at the 2-position of the benzodiazepine ring. Non-local information of this type can be taken into account by means of an extended transform. The extended transform is obtained by comparing the reactant, in this case K7/L2, of the reaction being modeled with the compound in the learning set, which is the most similar to this reactant but which does not undergo this reaction. For example (as shown in Fig. 6), to determine which compound of the learning set meets these requirements, K7/L2 is superimposed with every compound in the learning set and the compound containing the largest common structural fragment with K7/L2 is considered to be the most similar to K7/L2. Specifically, for the reaction of K7/L2 → L6, we compare compounds K7/L2 and K6 (Fig. 6). These two molecules are superimposed and the difference center is obtained. This difference center of the reactant is

Learning Set KL

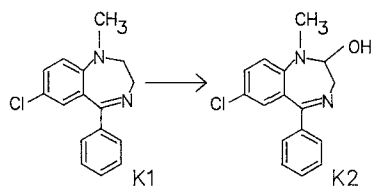

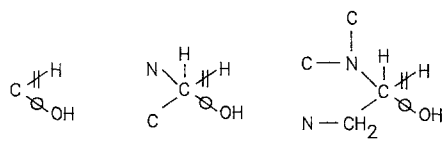

K1	1/9	1/2	1/1
K2	0/9	0/1	0/0
K4	0/7	0/0	0/0
K5	1/8	1/2	0/0
K6	0/8	0/1	0/0
K8	0/8	0/1	0/0
K9	0/6	0/0	0/0
K Total	2/55	2/7	1/1
L1	2/8	1/1	0/0
L2	2/7	1/1	0/0
L3	1/8	0/0	0/0
L5	1/7	1/1	0/0
L6	0/6	0/1	0/0
L7	0/7	0/0	0/0
L Total	6/43	3/4	0/0
KL Total	8/98	5/11	1/1

Fig. 5A. The sets of observed/predicted reactions for the KL learning dataset leading up to the selection of the complete 2-level transform constructed from the hydroxylation of K1.

considered essential for allowing the reaction being modeled to occur. The extended transform is constructed by connecting the reaction center and difference center (including that difference, i.e., C=O) by the shortest path of bonds through the molecule. The last column in Fig. 5D shows the performance of the extended transform describing the reaction K7/L2 → L6. All the reactions in the learning set are modeled using either a core, complete 1-level, complete 2-level, or extended transform.

A statistical evaluation of predictive performance

A method for determining the statistical significance of chemical transform prediction has also

Learning Set KL

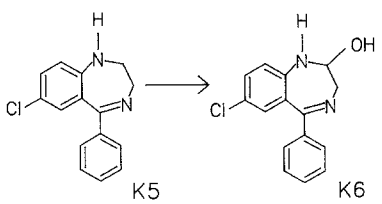

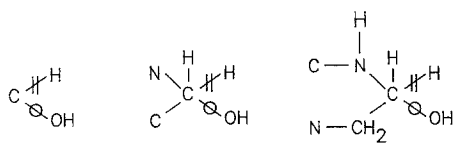

K1	1/9	1/2	0/0
K2	0/9	0/1	0/0
K4	0/7	0/0	0/0
K5	1/8	1/2	1/1
K6	0/8	0/1	0/0
K8	0/8	0/1	0/0
K9	0/6	0/0	0/0
K Total	2/55	2/7	1/1
L1	2/8	1/1	0/0
L2	2/7	1/1	0/0
L3	1/8	0/0	0/0
L5	1/7	1/1	0/0
L6	0/6	0/1	0/0
L7	0/7	0/0	0/0
L Total	6/43	3/4	0/0
KL Total	8/98	5/11	1/1

Fig. 5B. The sets of observed/predicted reactions for the KL learning dataset leading up to the selection of the complete 2-level transform constructed from the hydroxylation of K5.

been developed. Transformations can be grouped into one of 4 categories. Any envisioned chemical transformation may be predicted and observed, predicted but not observed, observed but not predicted, or neither observed nor predicted. This can be represented schematically by Fig. 7. Circle D represents all transformations generated by the core transforms. The union of circles B and C represent all reactions which are observed and/or predicted in the set. If we allow circle B to represent those reactions observed in the pathway and circle C to represent those reactions predicted by the transform kit, then the intersection of B and C will represent correct predictions of the transform kit. This intersection, labeled A, contains reactions which are predicted by the transform kit and observed in the chemical transformation pathway. The area labeled D, which

Learning Set KL

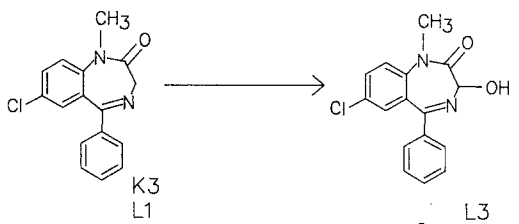

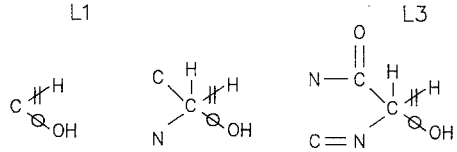

K1	1/9	1/2	0/0
K2	0/9	0/1	0/0
K4	0/7	0/0	0/0
K5	1/8	1/2	0/0
K6	0/8	0/1	0/0
K8	0/8	0/1	0/0
K9	0/6	0/0	0/0
K Total	2/55	2/7	0/0
L1	2/8	1/1	1/1
L2	2/7	1/1	1/1
L3	1/8	0/0	0/0
L5	1/7	1/1	1/1
L6	0/6	0/1	0/1
L7	0/7	0/0	0/0
L Total	6/43	3/4	3/4
KL Total	8/98	5/11	3/4

Fig. 5C. The sets of observed/predicted reactions for the KL learning dataset leading up to the selection of the complete 2-level transform constructed from the hydroxylation of K3/L1.

does not include A, B, or C, is the number of possible action sites of the core transforms of the kit minus the number of reactions accounted for by A, B, and C. This number, although large, is still smaller than the actual number of conceivable chemical transformations which may occur with a given set of compounds, but are neither observed nor predicted.

Various standard statistics [19] can be associated with a 2×2 table whose general form is given by Fig. 8. The phi association coefficient measures the agreement in the predicted and observed classification. The chi-square statistic tests if agreement can be entirely attributable to chance factors. In testing for a positive agreement, a chi-square greater than 2.71 would occur less than 5% of the time if only chance factors were operative. The sensitivity is the number of correct predictions (A) over the total number of observed reactions (A + B), and it estimates the proportion of

Learning Set KL

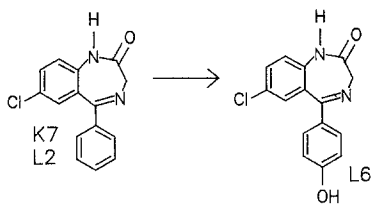

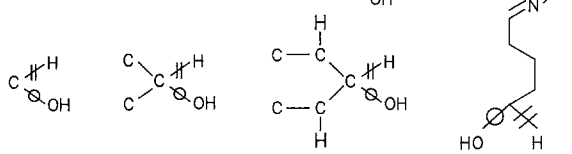

K1	1/9	0/6	0/2	0/0
K2	0/9	0/6	0/2	0/0
K4	0/7	0/6	0/2	0/0
K5	1/8	0/6	0/2	0/0
K6	0/8	0/6	0/2	0/0
K8	0/8	0/6	0/2	0/0
K9	0/6	0/6	0/2	0/0
K Total	2/55	0/42	0/14	0/0
L1	2/8	1/6	1/2	1/1
L2	2/7	1/6	1/2	1/1
L3	1/8	1/6	1/2	1/1
L5	1/7	0/5	0/0	0/0
L6	0/6	0/5	0/0	0/0
L7	0/7	0/5	0/0	0/0
L Total	6/43	3/33	3/6	3/3
KL Total	8/98	3/75	3/20	3/3

Fig. 5D. The sets of observed/predicted reactions for the KL learning dataset leading up to the selection of the extended transform constructed from the hydroxylation of K7/L2.

the time an event is predicted given it is observed. The specificity is the number of correct predictions (A) over the total number of predicted reactions (A + C), and it estimates the proportion of the time an event is observed given it is predicted.

Our learning algorithm includes in the kit a transform for each of the reactions in the learning set. These transforms are grouped and evaluated according to their associated core transforms (Fig. 9). For example, there are two different transforms included in the transform kit, both of which have the carboxyl-to-alcohol reduction as the core transform. These two transforms are evaluated for both the learning and testing data set using the core transform as the reference.

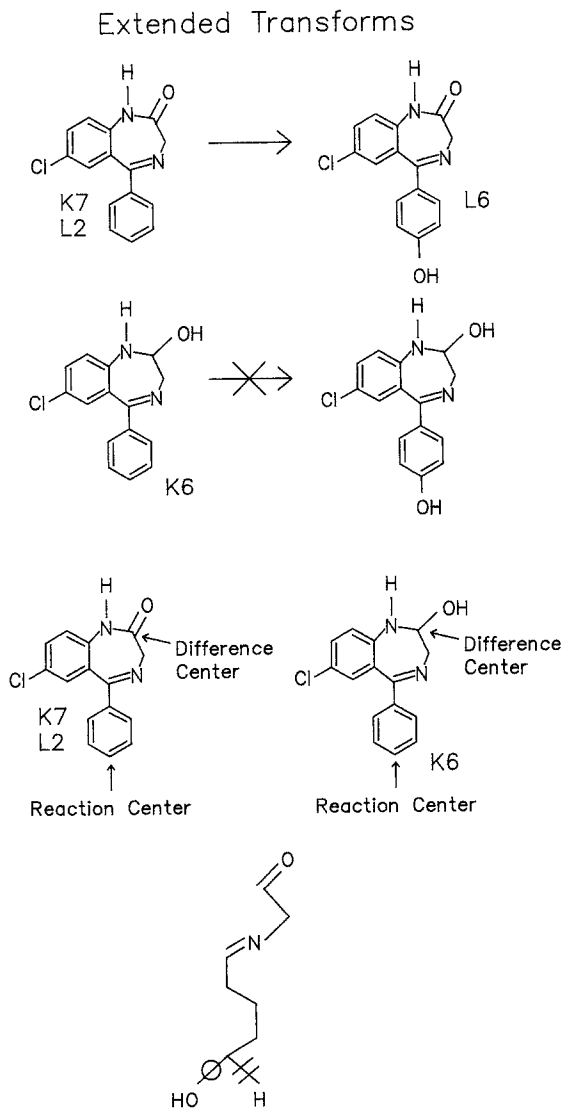

Fig. 6. The construction of the extended transform illustrating the difference between a compound (K7/L2) which undergoes para-hydroxylation and the most similar compound (K6) in the learning dataset which does not undergo para-hydroxylation.

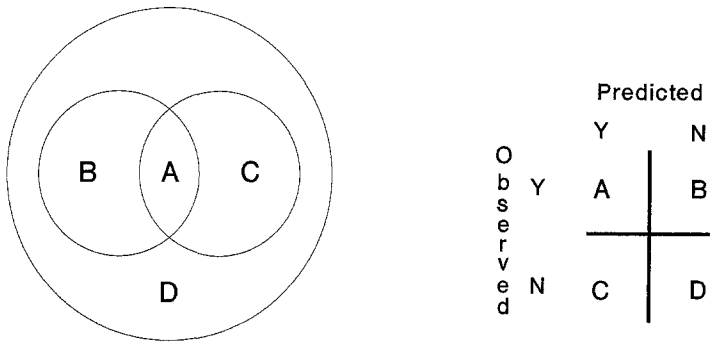

Fig. 7. A Venn diagram indicating the classification of distinguishable action sites of a core transform into the four possibilities: observed and predicted (A); observed but not predicted (B); not observed but predicted (C); and neither observed nor predicted (D).

The evaluation of the transform kit on the testing set must also include any reactions which are observed in the test set but not predicted by the transform kit, i.e., reactions unique to the testing set. These reactions are shown in Fig. 10. Since the structural environments of these reactions have not been determined, they may only be described by their core transform. The summation of all 2×2 tables, for the testing set, including those reactions unique to this set, is the 2×2 table used for an evaluation of the predictive ability of the transform kit. A similar summation is carried out for the learning set for comparative analysis.

The results of this pair-wise evaluation of our modeling of the medazepam (K), diazepam (L), and oxazepam (M) metabolic pathways are presented in Fig. 11. Each of the transform kits yields statistically significant results when applied to the corresponding testing set. These results are particularly striking given the limited size of the learning datasets and the primitive character of the learning algorithm, which was developed in a feasibility study on endogenous metabolism [20].

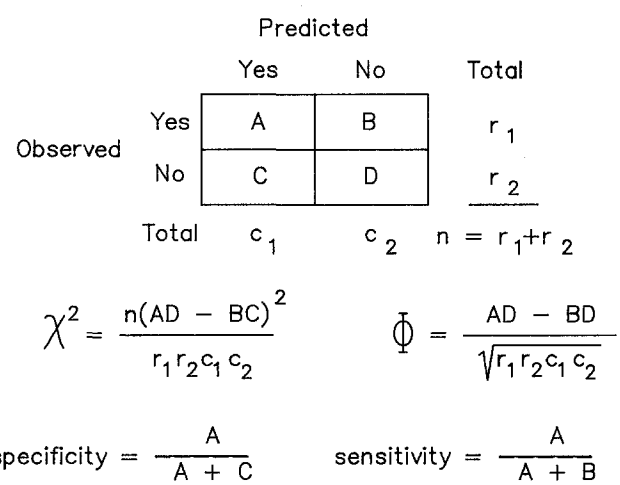

Fig. 8. The 2×2 table and statistics used to statistically evaluate the predictive capability of a transform.

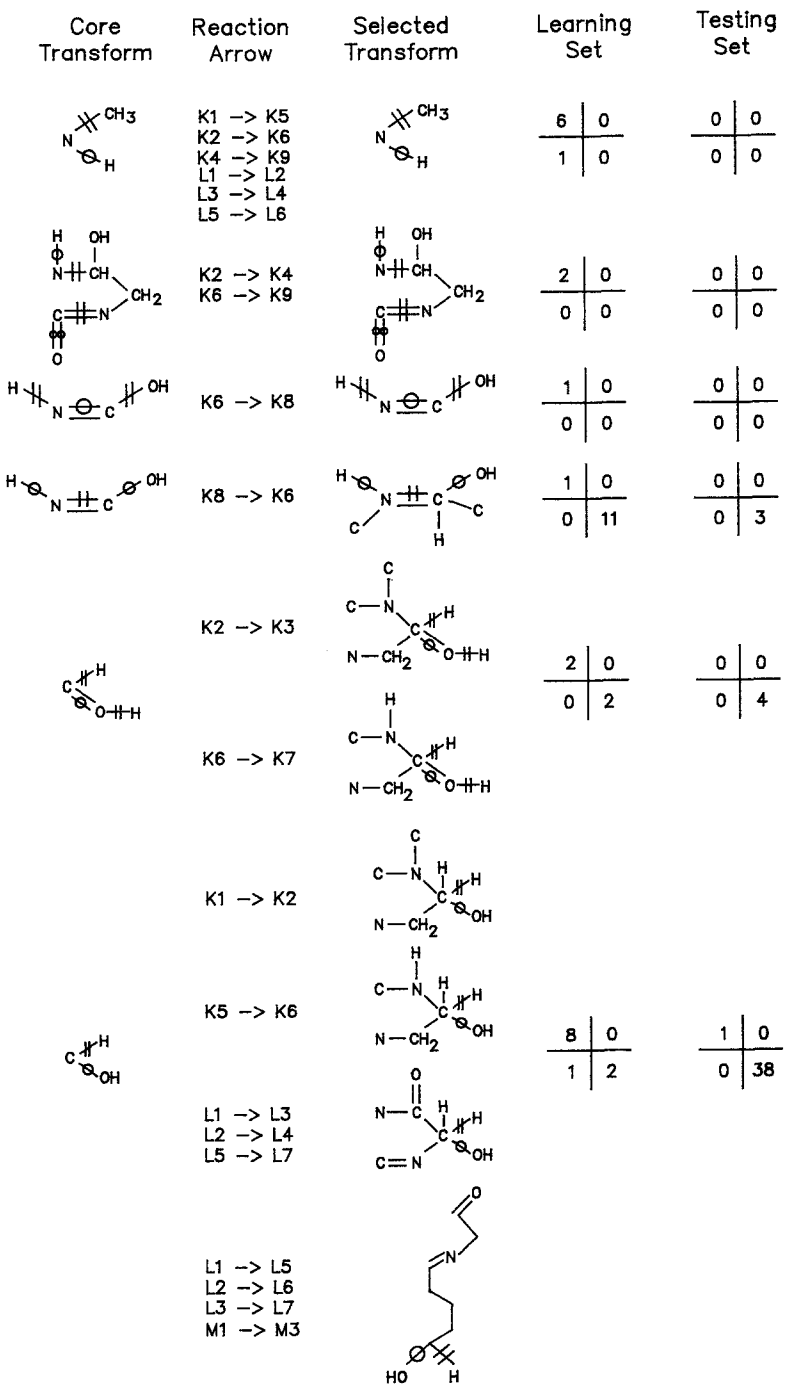

Fig. 9. The transforms of the transform kit constructed from the KL learning dataset. Each 2 × 2 table gives the predictive performance of the particular selected transform evaluated on the compounds in the learning dataset and in the testing dataset.

The best predictive result was obtained when using the KM learning dataset. The Φ coefficient was 0.64 for the testing dataset, vs. 0.39 and 0.27 in the other two cases. This is noteworthy because the parent molecule, diazepam, of the L testing dataset in this case lies 'structurally between' the two parent molecules, medazepam and oxazepam, of the K and M learning datasets. The concept of structural betweenness is defined explicitly in Ref. 21, but can be easily understood from Fig. 1, where we see that every R group of diazepam is possessed by either medazepam or oxazepam. This is not true for the other two compounds. Medazepam has a hydrogen for the R2 group which neither of the other two compounds has. Similarly, oxazepam has a hydroxyl group for the R3 group that neither of the other two compounds has. This raises the issue of predictions in an interpolative vs. an extrapolative sense. The importance of this concept is being investigated further.

PREDICTIVE PERFORMANCE ON OTHER BENZODIAZEPINES

The next phase of this project used the entire K, L, M pathway as a learning set. The transforms selected for inclusion in this kit (KLM learning kit) were obtained through the same procedure as previously described. This KLM learning kit was evaluated using 2×2 tables to determine how well this learning set was represented by the KLM learning kit. The results are shown in Fig. 12.

Core Transform	Reaction Arrow	Selected Transform	Learning Set	Testing Set
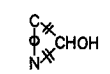	M1 –> M2		0 | 0 0 | 0	0 | 1 0 | 2
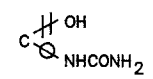	M4 –> M6		0 | 0 0 | 0	0 | 1 0 | 0
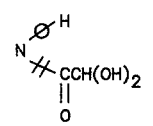	M4 –> M5		0 | 0 0 | 0	0 | 1 0 | 0
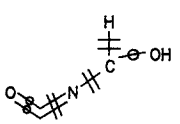	M1 –> M4		0 | 0 0 | 0	0 | 1 0 | 1
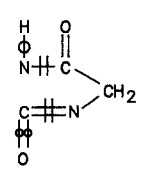	M1 –> M5		0 | 0 0 | 0	0 | 1 0 | 0

Fig. 10. The core transforms derived from reactions in the testing dataset (M), but not derivable from reactions in the learning dataset. The reactions represented by these core transforms are not observed in the learning dataset.

The KLM learning kit (Fig. 13) was then used to predict the first level of metabolites for the benzodiazepines, for which the published metabolic pathways are readily available [15]. These compounds are shown in Fig. 14. The first level of metabolites are those compounds which are either observed or predicted to be connected to the parent compound by one reaction arrow. Each of the compounds in Fig. 14 was individually subjected to the action of the KLM learning kit. Each transform in the KLM kit was allowed to act on each of the 16 compounds. The results for the first 3 compounds are given as an example (Fig. 15). The second column for each compound is the ratio of correct predictions to possible action sites of the transform. The third column is the number of possible action sites of the core transform on that compound. The transforms are grouped according to their core transforms. Transforms 1 through 4 have the same hydroxylation core transform that has 8 distinguishable sites on chlordiazepoxide. Transforms 5 and 6 have the same oxidation core transform that has no distinguishable sites on the first two compounds, but has one distinguishable site on lorazepam. The chi-square values for the 16 compounds ranged from 0.0227 to 12.00, and depended very much on the structure of the parent compound. The overall results for the KLM learning kit applied to these 16 compounds are shown in Fig. 16. It is encouraging that a statistically significant predictive result was obtained with a learning dataset consisting of the metabolic pathways of only three compounds.

DISCUSSION

This pilot study demonstrated that learning rules can be developed which generate transform giving regiospecific predictions of metabolic transformations in a closely related series of com-

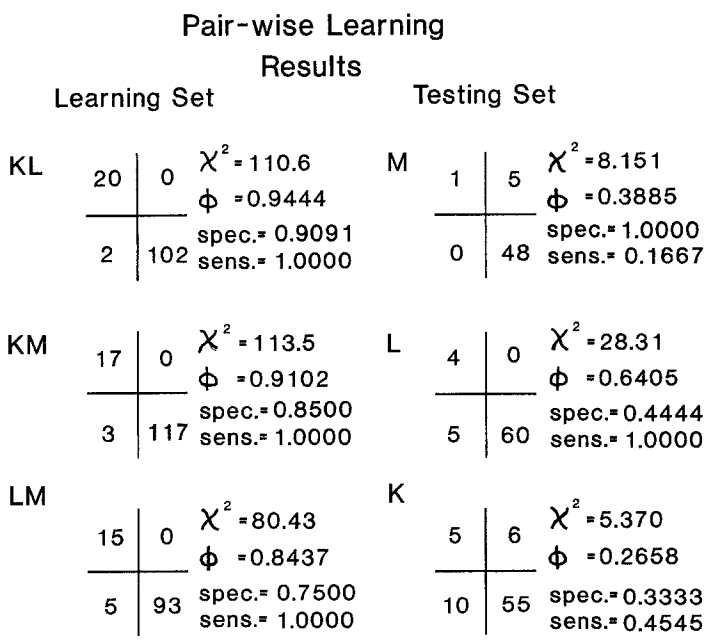

Fig. 11. A summary of the predictive performance of the transform kits constructed from the three learning datasets and evaluated against the corresponding testing datasets.

Core Transform	Number of Possible Reaction Sites	Number of Kit Predictions	Number of Correct Predictions	
	137	10	9	9 | 0 1 | 127
	8	2	2	2 | 0 0 | 6
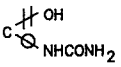	12	1	1	1 | 0 0 | 11
	7	2	1	1 | 0 1 | 5
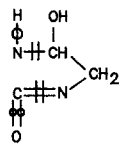	2	2	2	2 | 0 0 | 0
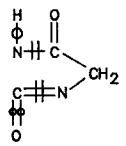	3	2	1	1 | 0 1 | 1
	7	7	6	6 | 0 1 | 0
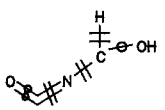	13	2	1	1 | 0 1 | 11
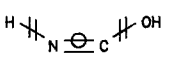	1	1	1	1 | 0 0 | 0
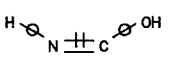	15	1	1	1 | 0 0 | 14
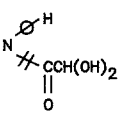	1	1	1	1 | 0 0 | 0

KLM Learning Kit Results

26	0	χ^2 = 168.0 ϕ = 0.9030
5	175	spec.= 0.8387 sens.= 1.0000

Fig. 12. The transform kit constructed from the combined learning dataset of Fig. 2 (KLM learning dataset) and the evaluation summary.

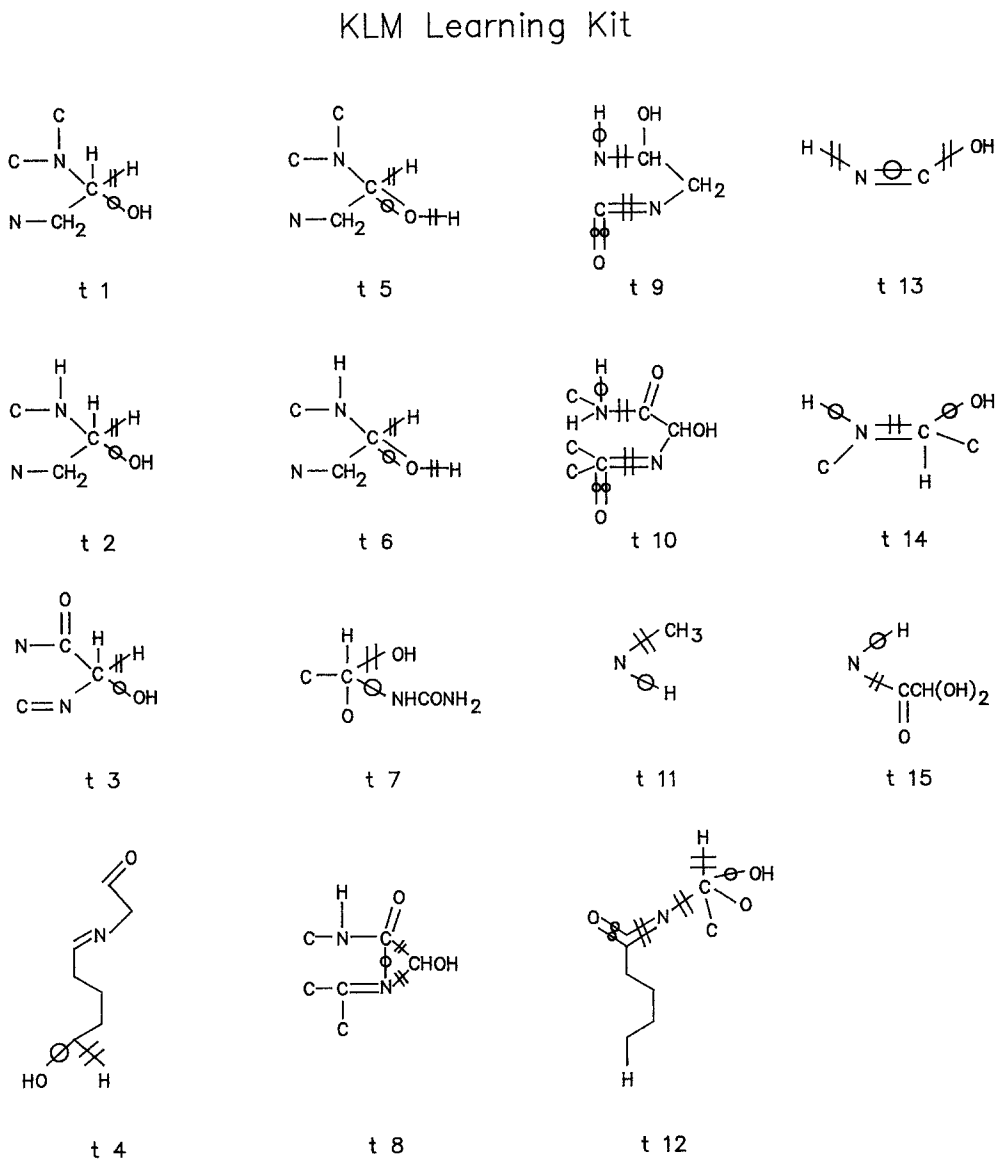

Fig. 13. The actual transform kit used to model the reactions in Fig. 2 (KLM learning dataset).

pounds. Although this regiospecificity was only established for a closely related series of compounds, the generated transforms are operational on any compound. Thus, operationally, the predictive method is not limited to related series of compounds in the way that substituent-based methods are limited to series of compounds with a common skeleton. It is a nice feature of the formalism underlying this study, that the generated transforms are both interpretable and visual. Moreover, the 2×2 tables associated with each transform enable one to quickly evaluate the performance of the transform as well as the amount of data on which this performance is based.

This study also suggests a number of ways in which predictive performance may be improved.

Conditions under which two transforms may be advantageously replaced by a single transform consisting of the commonality of the two transforms were already noted in the section on selection of appropriate transforms. If one examines more closely the cases in which the generated transforms failed to predict an observed transform, one can see how performance can be enhanced by using larger learning datasets. Clearly, compounds which have functional groups not observed in the learning set may undergo reactions which will not have been modeled. For example, one of the first-level metabolic reactions of nitrazepam is the reduction of the nitro group to

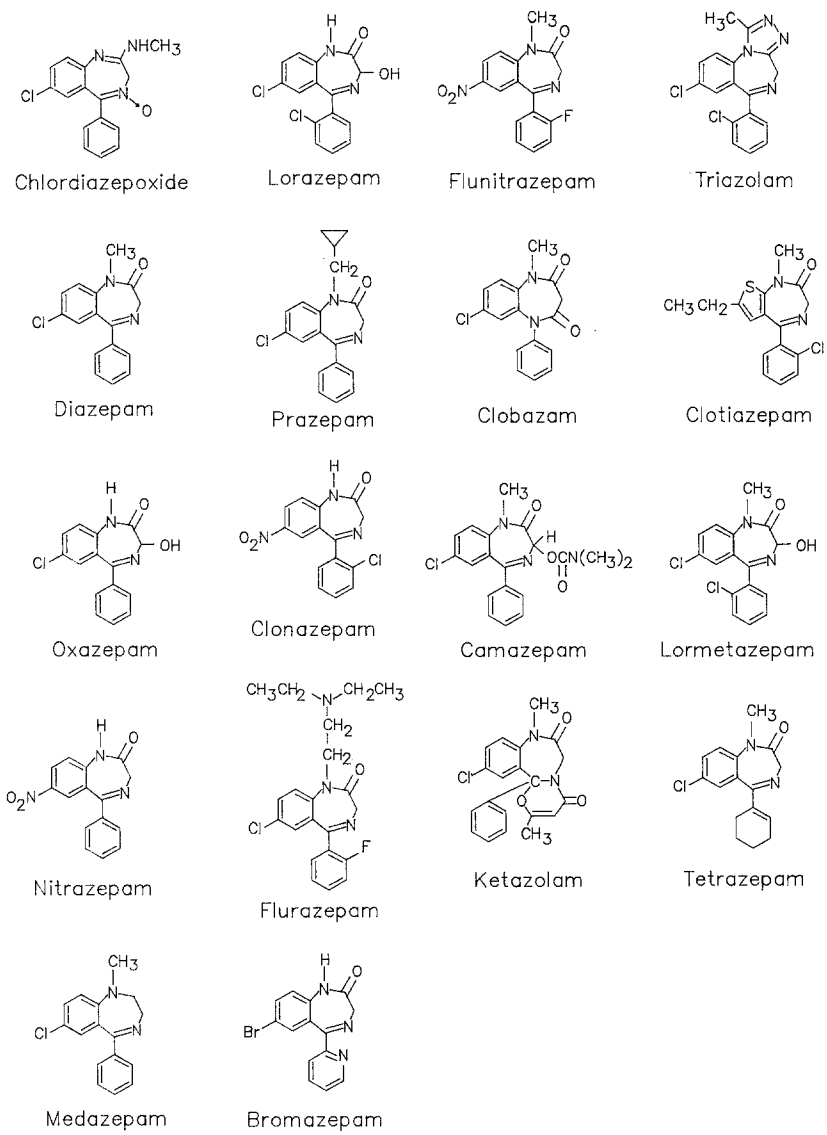

Fig. 14. The benzodiazepines whose first-level metabolic reactions are to be predicted using the KLM transform kit in Fig. 13.

KLM Learning Kit

	Chlordiazepoxide		Nitrazepam		Lorazepam	
t 1	0/0	8	0/0	7	0/0	7
t 2	0/0	–	0/0	–	0/0	–
t 3	0/0	–	0/1	–	0/0	–
t 4	0/0	–	0/1	–	1/1	–
t 5	0/0	0	0/0	0	0/0	1
t 6	0/0	–	0/0	–	0/0	–
t 7	0/0	0	0/0	0	0/0	0
t 8	0/0	0	0/0	0	1/1	1
t 9	0/0	0	0/0	0	0/0	0
t 10	0/0	0	0/0	0	1/1	1
t 11	1/1	1	0/0	0	0/0	0
t 12	0/0	0	0/0	0	0/1	1
t 13	0/0	0	0/0	0	0/0	0
t 14	0/0	1	0/0	1	0/0	1
t 15	0/0	0	0/0	0	0/0	0

1	0		0	2	3	0
0	9		2	4	1	8

χ^2 = 10.00
ϕ = 1.0000
spec.= 1.0000
sens.= 1.0000

χ^2 = 0.8889
ϕ = 0.3333
spec.= 0.0000
sens.= 0.0000

χ^2 = 8.0000
ϕ = 0.8165
spec.= 0.7500
sens.= 1.0000

Fig. 15. The performance of each transform in the KLM transform kit evaluated against the first-level metabolic reactions of chlordiazepoxide, nitrazepam, and lorazepam.

a primary amine. This reaction was not predicted since the nitro group does not appear on any compound in the KLM learning set. The same is true for the acetylation of the primary amine. Of the 20 reactions that were observed but not predicted, 11 involved functional groups not found in the KLM learning dataset. If one eliminates these 11 missed predictions from the computation of the sensitivity in Fig. 16, this sensitivity jumps from 41% to 60%. Clearly, as larger learning data-

KLM Learning Kit

Results Summary

14	20	χ^2 = 14.26
		ϕ = 0.2784
20	130	spec.= 0.4118
		sens.= 0.4118

Kit Applied to Parent Compounds
of Benzodiazepine Data Set

Fig. 16. The predictive performance of the KLM transform kit evaluated against the first-level metabolic reactions of the compounds in Fig. 14.

sets become available and more sophisticated learning rules are developed, dramatic enhancements to the predictive performance of the generated kits can be expected. Thus, in a roundabout-way, this study suggests that general regiospecific computer-assisted metabolic prediction may become a reality with the advent of extensive databases of metabolic transformations.

ACKNOWLEDGEMENTS

We would like to thank Gerald Maggiora, director of Computational Chemistry at Upjohn Laboratories, for providing the opportunity for Eric Gifford to perform much of this work as a summer employee.

REFERENCES

1 Bodor, N., Trends Pharm. Sci., 3 (1982) 53.
2 Caldwell, J. and Hutt, A.J., In Caldwell, J. and Paulson, G.D. (Eds.), Foreign Compound Metabolism, Taylor & Francis, London, 1984, pp. 101–108.
3 Case, D.E., In Caldwell, J. and Paulson, G.D. (Eds.), Foreign Compound Metabolism, Taylor & Francis, London, 1984, pp. 119–122.
4 Barcza, S., Kelly, L.A. and Lenz, C.D., J. Chem. Inf. Comput. Sci., 30 (1990) 243.
5 Darvas, F., J. Mol. Graphics, 6 (1988) 80.
6 Lindsay, R.K., Buchanan, B.G., Feigenbaum, E.A. and Lederberg, J., Applications of Artificial Intelligence for Organic Chemistry: The Dendral Project, McGraw-Hill Book Co., New York, 1980.
7 Wilcox, C.S. and Levinson, R.A., In Pierce, T.H. and Hohne, B.A. (Eds.), Artificial Intelligence Applications in Chemistry (ACS Symposium Series 306) American Chemical Society, Washington, DC, 1986, pp. 209–230.
8 Yanaka, M., Nakamura, K., Kurumisawa, A. and Wipke, W.T., In Fauch'ere, J.L. (Ed.), QSAR: Quantitative Structure–Activity Relationships in Drug Design, Alan R. Liss, Inc., New York, 1989, pp. 147–150.
9 Johnson, M.A., Gifford, E. and Tsai, C.-C., In Johnson, M.A. and Maggiora, G.M. (Eds.), Concepts and Applications of Molecular Similarity, John Wiley & Sons, New York, 1990, pp. 289–320.
10 Zou, Y., Johnson, M.A. and Tsai, C.-C., J. Chem. Inf. Comput. Sci., (1991) in press.
11 Wipke, W.T., Ouchi, G.I. and Chou, J.T., In Goldberg, L. (Ed.), Structure–Activity Correlations as Predictive Tools in Toxicology, Hemisphere Publishing Co., Washington, DC, 1983, pp. 151–169.
12 Tinker, J.F. and Gelernter, H., J. Comput. Chem., 7 (1986) 657.
13 Hansch, C., Drug Metab. Rev., 1 (1972) 1.
14 Hollister, L.E., Clinical Pharmacology of Psychotherapeutic Drugs, 2nd edn., Churchill Livingstone, New York, 1983.
15 Schutz, H., Benzodiazepines, Springer-Verlag, Berlin, 1982.
16 Testa, B. and Jenner, P., Drug Metabolism: Chemical and Biochemical Aspects, Marcel Dekker, New York, 1976.
17 Fujita, S., J. Chem. Inf. Comput. Sci., 26 (1986) 205.
18 Fujita, S., J. Chem. Inf. Comput. Sci., 27 (1987) 120.
19 Conover, W.J., Practical Nonparametric Statistics, John Wiley & Sons, New York, 1980.
20 Johnson, M., Gifford, E. and Tsai, C.-C., In Johnson, M.A. and Maggiora, G.M. (Eds.), Concepts and Applications of Molecular Similarity, John Wiley & Sons, New York, 1990, pp. 289–320.
21 Johnson, M., Naim, M., Nicholson, V. and Tsai, C.-C., In King, R.B. and Rouvray, D.H. (Eds.), Graph Theory and Topology in Chemistry, Elsevier, Amsterdam, 1987, pp. 219–225.